CN 51-1346/O4 ISSN 1003-501X (印刷版) ISSN 2094-4019 (网络版)

光电工程
Opto-Electronic Engineering

中文核心期刊 中国科技核心期刊
Scopus CSCD

基于单光束矢量光场调控的紧聚焦均匀三维光泡的产生与探测

郑泽灿，王思聪，冯嘉浩，周志凯，陈树康，宋世超，邓子岚，秦飞，曹耀宇，李向平

引用本文:

郑泽灿，王思聪，冯嘉浩，等. 基于单光束矢量光场调控的紧聚焦均匀三维光泡的产生与探测[J]. 光电工程，2025，**52**(5): 250052.

Zheng Z C, Wang S C, Feng J H, et al. Generation and detection of a tightly focused uniform optical bubble based on single-beam vector field modulation[J]. *Opto-Electron Eng*, 2025, **52**(5): 250052.

https://doi.org/10.12086/oee.2025.250052

收稿日期: 2025-02-24; 修改日期: 2025-04-29; 录用日期: 2025-04-30

相关论文

Opto-Electronic Engineering
光 电 工 程

Article

2025 年, 第 52 卷, 第 5 期

DOI: 10.12086/oee.2025.250052 CSTR: 32245.14.oee.2025.250052

基于单光束矢量光场调控的紧聚焦均匀三维光泡的产生与探测

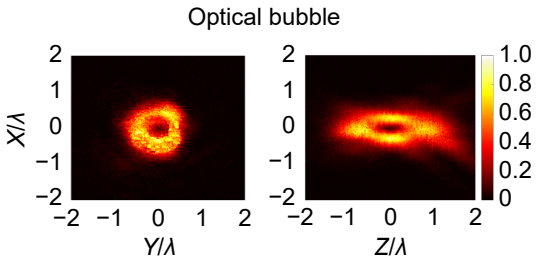

郑泽灿，王思聪*，冯嘉浩，周志凯，陈树康，宋世超，邓子岚，秦 飞，曹耀宇，李向平

暨南大学物理与光电工程学院，光子技术研究院，广东省光纤传感与通信技术重点实验室，广东 广州 510632

摘要：三维光泡，即紧聚焦三维中空暗场光斑分布，在光学操控以及激光加工等领域中具有重要的应用价值。在已报道的工作中，三维光泡一般采用多光束干涉叠加的方式来产生，光路复杂，不利于系统集成应用，且能量利用率低。利用单光束矢量光场调控技术，产生高强度均匀性紧聚焦三维光泡，并利用探测光偏振转换技术实现对三维光泡的探测。通过调节旋向偏振入射光与 0/π 二元相位调制的径向偏振入射光的能量比，在实验上实现边缘强度与中心暗斑强度比值大于 10:1、边缘强度均匀度接近 90% 的三维光泡，为双光束超分辨激光加工与光存储、粒子操控等领域提供实用的技术途径。

关键词：矢量光场调控；三维光泡；纵向偏振分量探测

中图分类号：O436 **文献标志码：**A

郑泽灿，王思聪，冯嘉浩，等. 基于单光束矢量光场调控的紧聚焦均匀三维光泡的产生与探测 [J]. 光电工程，2025，**52**(5): 250052

Zheng Z C, Wang S C, Feng J H, et al. Generation and detection of a tightly focused uniform optical bubble based on single-beam vector field modulation[J]. *Opto-Electron Eng*, 2025, **52**(5): 250052

Generation and detection of a tightly focused uniform optical bubble based on single-beam vector field modulation

Zheng Zecan, Wang Sicong*, Feng Jiahao, Zhou Zhikai, Chen Shukang, Song Shichao, Deng Zilan, Qin Fei, Cao Yaoyu, Li Xiangping

Guangdong Provincial Key Laboratory of Optical Fiber Sensing and Communications, Institute of Photonics Technology, College of Physics & Optoelectronic Engineering, Jinan University, Guangzhou, Guangdong 510632, China

Abstract: Optical bubble, characterized by a tightly focused three-dimensional dark-field intensity distribution, exhibits significant application value in fields such as optical manipulation and laser processing. In previously reported results, an optical bubble is typically generated through multi-beam interference and superposition, which

收稿日期：2025-02-24；修回日期：2025-04-29；录用日期：2025-04-30

基金项目：国家重点研发计划 (2023YFF0718101)；国家自然科学基金 (62375109, 62475102, 62275108)

*通信作者：王思聪，wangsc@jnu.edn.cn。

involves complex optical setups and is not conducive to system integration and practical applications, and has low energy utilization efficiency. In this study, we utilize single-beam vector field modulation technology to generate a tightly focused optical bubble with high intensity uniformity. Furthermore, we achieve the detection of this hollow bubble through polarization conversion of the probe light. By adjusting the energy ratio between azimuthally polarized incident beam and radially polarized incident beam modulated by a 0/π binary phase, we experimentally realize an optical bubble with an edge-to-center dark spot intensity ratio exceeding 10:1 and edge intensity uniformity approaching 90%. This work provides a feasible technical approach for applications in dual-beam super-resolution laser processing, optical data storage, and particle manipulation.

Keywords: vector light field modulation; three-dimensional optical bubble; longitudinal polarization component detection

1 引　言

矢量光场是指在同一时刻、同一波阵面、不同空间位置上具有不同偏振态分布的光场。其中，柱对称矢量光场 (例如径向偏振光场、旋向偏振光场等) 是最典型的一类矢量光场分布[1-2]。区别于传统的标量光场，矢量光场具有更为独特的紧聚焦特性并得到人们的广泛关注。例如，旋向偏振入射光在紧聚焦时能够生成中空甜甜圈状光场分布 (doughnut)，而径向偏振入射光在紧聚焦条件下能够产生极强的纵向电场分量，进而生成小尺度聚焦光斑。当前，各类先进的矢量光场调控技术已实现丰富多样的功能型结构光场分布[3]，在光学、生物学[4]、材料学[5] 等多学科研究领域中具有巨大的潜在应用价值。

相较于中空二维甜甜圈状光场分布，三维光泡 (optical bubble) 在空间三维超分辨光学显微成像[6-8]、纳米加工[9-15]、光存储[16-18]、纳米粒子操纵[19-20] 等领域中具有更为广阔的应用前景。自 2000 年以来，人们便开始三维光泡聚焦光场分布的研究。Arlt 等[21] 利用两种不同模式的拉盖尔-高斯光束相干叠加在聚焦空间中产生三维光泡；Chen 等[22] 利用柱矢量光束并结合二元衍射光学元件产生紧聚焦三维光泡；Kozawa 等[23] 利用双环形径向偏振光束相干叠加产生三维光泡。然而，以上方法生成的三维光泡边缘光场强度分布均匀性较差，影响其实际应用效果。在粒子操控方面，高均匀性光泡可形成对称且梯度平缓的力场，减少局部力场畸变，使粒子 (如生物细胞、纳米颗粒) 在光阱中被更精准地捕获，避免力场不均匀导致粒子逃逸。均匀能量分布也可避免局部过热，减少激光对热敏感粒子 (如活体细胞) 的损伤，提高实验的可控性和重复性；在加工精度方面，高均匀性光泡使双光束干涉形成的能量分布更均匀，可在材料表面或内部形成规则的微结构 (如光子晶体、微孔阵列)，避免能量不均匀导致加工深度不一或边缘毛刺，提高加工成品率。为解决这一问题，Bokor 等[24] 利用拉盖尔-高斯型的径向偏振光束进行 4π 聚焦，在聚焦空间中生成高强度均匀性的三维光泡。但相向传播聚焦的 4π 聚焦模式需要较高的实验操作精度，难以在实验上实现。随后，该课题组在传统单向聚焦条件下，通过调节旋向偏振入射光与 0/π 二元相位调制的径向偏振入射光的能量比，构造产生了高强度均匀性的三维光泡[25]。然而，目前人们均利用多光束合成的方式在实验上生成光泡[26]，对实验系统的搭建 (特别是多脉冲光束合成系统) 提出了较高要求，且系统能量利用率较低。对以上方法及效果进行归纳对比，如表 1 所示。

针对这一问题，发展了单光束矢量光场调控技术，在简易实验系统中产生高强度均匀性、高能量利用率的三维光泡。进一步，利用探测光偏振转换技术实现对聚焦场各偏振分量的探测，并合成了三维光泡的形貌分布。本工作将为双光束超分辨激光加工与光存储、粒子操控等领域提供更为实用的技术途径。

2 理论模拟

当径向偏振光束被高数值孔径消球差透镜紧聚焦时，根据 Richards-Wolf 矢量衍射理论[27-29]，聚焦场的径向偏振分量E_r和纵向偏振分量E_z分别表示为

$$E_{\mathrm{r}}(r_{\mathrm{p}},\phi_{\mathrm{p}},z_{\mathrm{p}})=A_{\mathrm{r}}\int_0^{\theta_{\max}} l_0(\theta)\times \mathrm{J}_1(kr_{\mathrm{p}}\sin\theta)\cos\theta \mathrm{e}^{\mathrm{i}kz_{\mathrm{p}}\cos\theta} \times\sqrt{\cos\theta}\sin\theta \mathrm{d}\theta, \tag{1}$$

$$E_z(r_{\mathrm{p}},\phi_{\mathrm{p}},z_{\mathrm{p}})=A_{\mathrm{r}}\int_0^{\theta_{\max}} l_0(\theta)\times \mathrm{i}\mathrm{J}_0(kr_{\mathrm{p}}\sin\theta)\sin\theta \mathrm{e}^{\mathrm{i}kz_{\mathrm{p}}\cos\theta} \times\sqrt{\cos\theta}\sin\theta \mathrm{d}\theta, \tag{2}$$

表 1 三维光泡产生方法及效果对比

Table 1 Comparison of three-dimensional optical bubble generation methods and effects

编号	文章信息	方法	原理图	聚焦光强分布 (*XZ*面)	均匀度	存在的问题
1	J. Arlt, et al., Opt. Lett. 25, 191 (2000).	两种不同模式的拉盖尔-高斯光束紧聚焦	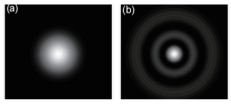	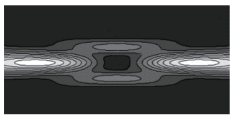	低于 50%	强度分布均匀性较差
2	W.Chen, et al., Opt.Commun. 265, 411 (2006).	柱矢量光束并结合二元衍射光学元件	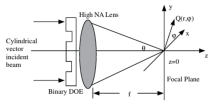	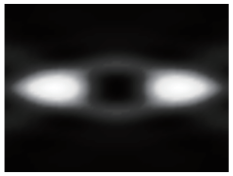	低于 50%	强度分布均匀性较差
3	Y.Kozawa, et al., Opt. Lett. 31, 820 (2006).	双环形径向偏振光紧聚焦	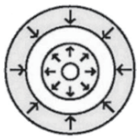	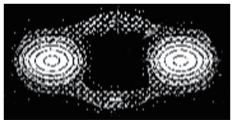	低于 50%	强度分布均匀性较差
4	N.Bokor, et al., Opt. Lett. 31, 149 (2006).	两个反向传播的径向偏振 LG 光束 4π 聚焦	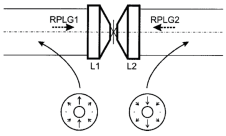	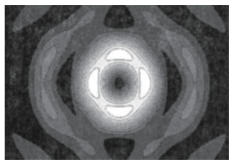	接近 90%	4π 聚焦实验较难实现
5	N.Bokor, et al., Opt.Commun. 279, 229 (2007).	旋向偏振光与 0/π 二元相位调制的径向偏振光叠加合成聚焦	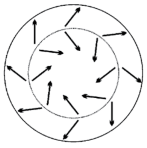	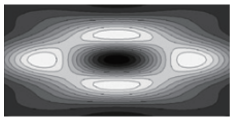	接近 90%	实验上利用多光束合成实现, 能量利用率较低

$$l_0(\theta)=\exp\left[-\beta_0^2\left(\frac{\sin\theta}{\sin\theta_{\max}}\right)^2\right]\mathrm{J}_1\left(2\beta_0\frac{\sin\theta}{\sin\theta_{\max}}\right). \quad (3)$$

当旋向偏振光束被高数值孔径消球差透镜紧聚焦时，聚焦场的旋向偏振分量E_Φ表示为

$$E_\Phi(r_\mathrm{p},\phi_\mathrm{p},z_p)=A_\Phi\int_0^{\theta_{\max}} l_0(\theta)\times\mathrm{J}_1(kr_\mathrm{p}\sin\theta)\mathrm{e}^{\mathrm{i}kz_\mathrm{p}\cos\theta}\times\sqrt{\cos\theta}\sin\theta\mathrm{d}\theta \quad , \quad (4)$$

式中：$(r_\mathrm{p},\phi_\mathrm{p},z_\mathrm{p})$是聚焦空间的柱坐标；$A_\mathrm{r}$和$A_\Phi$是常数；$\beta_0$是透镜孔径与光束光腰的比值，$\beta_0=1.5$；$k$是聚焦空间中波矢的大小；$\theta$是入射光各空间频谱与光轴的夹角；$\theta_{\max}$是最大空间频谱会聚角，$\theta_{\max}=\arcsin(NA/n')$，其中数值孔径$NA=1.4$ (油镜)，聚焦空间折射率$n'=1.515$；J_0和J_1分别是零阶和一阶第一类贝塞尔函数。

旋向偏振入射光紧聚焦光场呈现以光轴为对称轴的中空管状分布 (如图 1(a) 所示)；径向偏振入射光则通过 0/π 二元相位调制，其中二元相位板内外环半径分别为R_i和R_o(如图 1(b) 所示)，调节$R_\mathrm{i}:R_\mathrm{o}$比值为 0.218:1，可使得聚焦场纵向电场分量在聚焦空间中心区域相干相消从而形成暗场，并沿光轴在焦平面两侧相干相长。进一步，叠加两聚焦光场，即可生成三维光泡 (如图 1(c) 所示)。

通过调节旋向偏振入射光与径向偏振入射光的能量比，可获得具有不同聚焦光场强度均匀度$\Phi=\frac{II_{\min}}{II_{\max}}$的三维光泡。其中，$II$是以聚焦中心为原点，沿包含光轴的 *XZ* 平面内各个方向的最大光强的集合。定义沿 *c* 方向时，光场强度的最大值为$II_{\min}$。如图 1(d) 所示，通过计算可得，当旋向偏振入射光与径向偏振入射光的能量比为 1:1.4 时，可以获得最佳的均匀度 (Φ= 91.1%)。图 1(a) 为旋向偏振入射光紧聚焦光斑在 *XY* 焦平面和 *XZ* 平面内的光场强度归一化分布，图 1(b) 为 0/π 二元相位调制的径向偏振入射光紧聚焦光斑在 *XY* 焦平面和 *XZ* 平面内的光场强度归一化分布，图 1(c) 表示在最佳强度均匀度时，叠加生成的三维光泡在 *XY* 焦平面和 *XZ* 平面内的光场强度归一化分布。图 1(e) 是三维光泡沿 *x* 方向、*z* 方向和 *c* 方向的光场强度归一化曲线。可以得出，三维光泡光场强度沿 *x* 方向，*z* 方向和 *c* 方向的中心暗场半峰高全宽 (FWHM) 分别为：$FWHM_x$=0.305 λ，$FWHM_z$=0.887 λ，$FWHM_c$=0.305 λ (λ 为激光波长)。

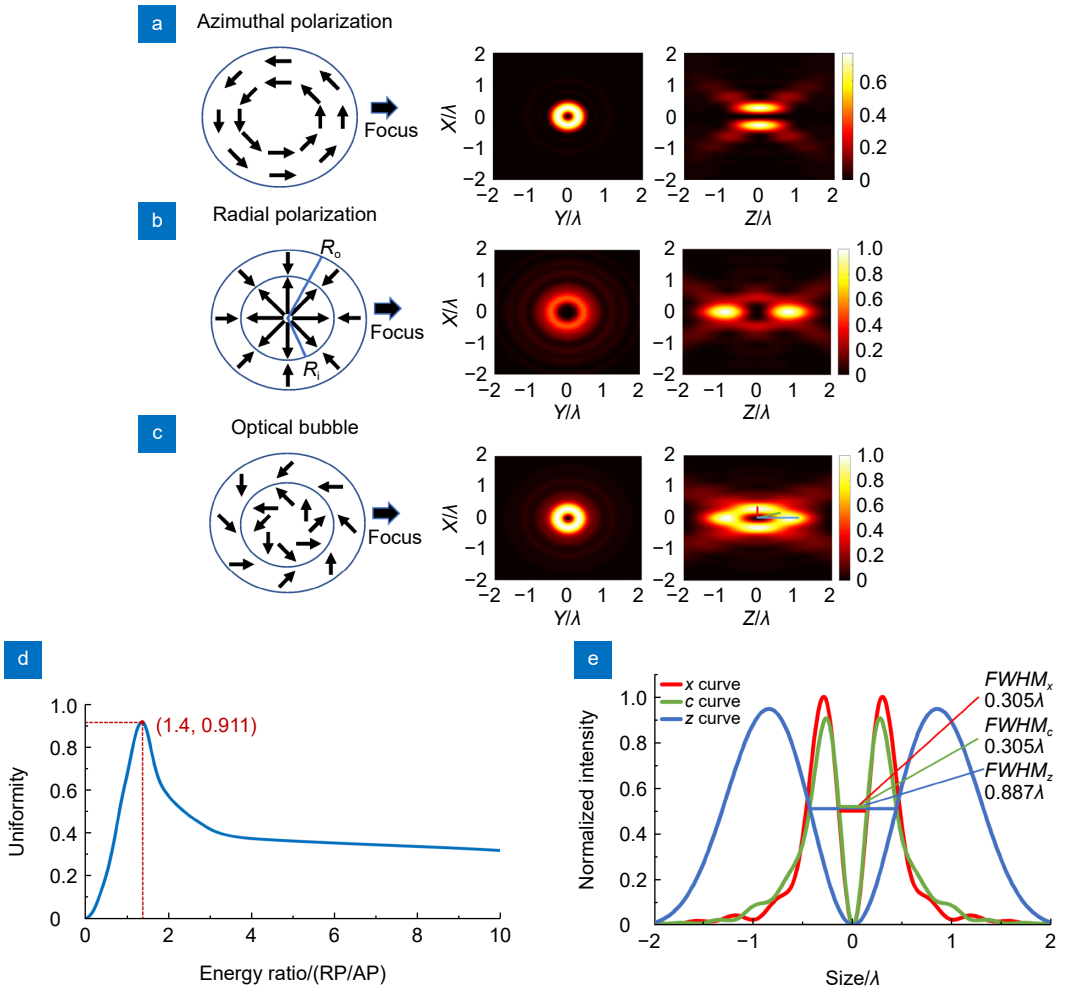

图 1 *XY* 焦平面和包含光轴的 *XZ* 平面内的光场强度归一化分布和三维光泡的光场强度归一化曲线理论结果。(a) 旋向偏振入射光紧聚焦生成中空管状光场；(b) 0/π 二元相位调制的径向偏振入射光紧聚焦光场；(c) 在最佳强度均匀度时，二者叠加生成的紧聚焦三维光泡；(d) 不同能量比下 (RP/AP) 三维光泡均匀度变化曲线图；(e) 三维光泡沿 *x* 方向、*z* 方向和 *c* 方向的光场强度归一化曲线

Fig. 1 Normalized intensity distributions of optical field intensity in *XY* focal plane and *XZ* plane containing the optical axis, as well as theoretical results of normalized intensity curves of three-dimensional optical bubble. (a) Tightly focused hollow tubular optical field generated by azimuthally polarized incident beam; (b) Tightly focused optical field generated by radially polarized incident beam with 0/π binary phase modulation; (c) Tightly focused three-dimensional optical bubble generated by superposition of two under optimal intensity uniformity; (d) Variation curve of three-dimensional optical bubble uniformity under different energy ratios (RP/AP); (e) Normalized intensity curves of three-dimensional optical bubble along *x*-direction, *z*-direction, and *c*-direction

3 实验产生与探测

如图 2 所示，利用单光束矢量光场调控技术，通过高数值孔径物镜 (*NA*=1.4) 紧聚焦生成三维光泡。其中，空间光调制器 (spatial light modulator, SLM, PLUTO 1) 仅对某一特定偏振取向的线偏振 (例如水平或竖直偏振) 入射光进行相位调制，而对与其正交的偏振分量不作任何调制。通过改变入射至 SLM 光束的线偏振态取向，便可改变两正交偏振分量的能量比。随后，两正交偏振分量同时入射至径向/旋向偏振转换器 (radial polarization converter, RPC, RADPOL4)，并分别转换为径向偏振光与旋向偏振光，其中径向偏振光携带 SLM 所施加的 0/π 二元相位调制。在特定偏压下，偏振转换器只对竖直偏振分量进行 0/π 相位补偿，并进一步偏振转换为旋向偏振光，而无法对水平偏振分量进行相位补偿。因此，需要在 SLM 上额外加载上下 0/π 相位，对水平偏振分量进行相位补偿，并生成径向偏振光。进一步，叠加 0/π 环形相位调制使得聚焦场纵向电场分量在聚焦空间中心区域相干相消从而形成暗场。叠加后的调制相位分布如图 2 插

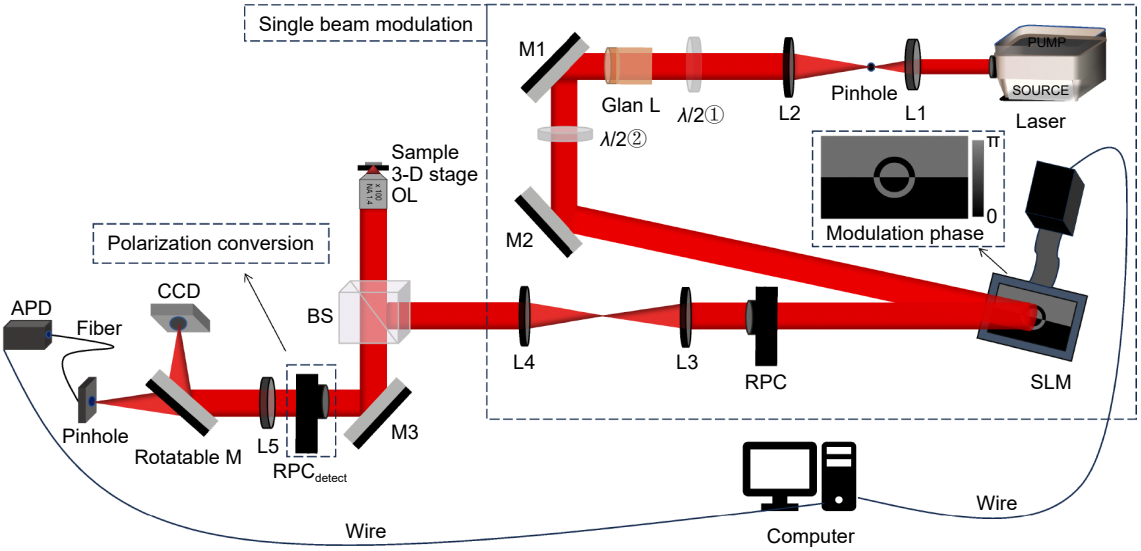

L1, L2, L3, L4, L5: convex lens; M1, M2, M3: rotatable M:reflecting mirror; λ/2①, λ/2②: half waveplate; Glan L: Glandtl prism; BS: beam splitter; CCD: charge coupled device; RPC, RPCdetect: radial polarization converter; SLM: spatial lightmodulator; APD: Avalanche photodiode, OL: Objective lens

图 2 基于单光束矢量光场调控和金纳米颗粒扫描的紧聚焦三维光泡的产生和探测光路示意图

Fig. 2 Optical path schematic for the generation and detection of a tightly focused optical bubble based on single-path vector beams manipulation and gold nanoparticle scanning

图所示。本实验方案大幅度降低了实验光路系统的搭建难度，特别是针对脉冲光束，可以有效规避多光束合束所带来的光程补偿问题。本实验采用波长为 687 nm、重复率为 80 MHz、脉宽为 140 fs 的飞秒激光光源 (coherent chameleon ultra)。进一步，本实验利用金纳米颗粒扫描方法[17,30-32] 对所产生的紧聚焦三维光泡进行扫描探测。其中，金纳米颗粒样品直径为 100 nm，由商用金颗粒溶液稀释制备而成。金纳米颗粒的散射光被同一物镜收集，并传输至雪崩光电二极管 (avalanche photo diode, APD, SPCM-AQRH-14-FC)。由于远场探测方式无法直接探测到聚焦光场的纵向偏振分量 E_z，需要利用探测光偏振转换技术来实现 E_z 的间接测量。具体而言，聚焦光场的纵向偏振分量在远场收集时会变成径向偏振光，而径向偏振光通过低数值孔径透镜 (tube lens) 聚焦后，将呈现中空甜甜圈状光斑分布而无法被 APD 收集。为此，在探测光路中安放另一偏振转换器 (RPC$_{detect}$)，将径向偏振光转换成线偏振光，再通过低数值孔径透镜聚焦，并被 APD 收集。利用此种偏振转换技术，实现了聚焦光场纵向偏振分量的间接测量[33]。为了尽量提高测量结果的准确性，调节旋向偏振入射光与径向偏振入射光的能量比为 1:1.4，即在最佳聚焦光场强度均匀度条件下，分别对旋向偏振光聚焦光场 (纯旋向偏振分量) 和 0/π 二元相位调制的径向偏振光聚焦光场 (纵向偏振分量占主导) 进行测量。在测量旋向偏振光聚焦光场时，探测光路中不安放 RPC$_{detect}$。

图 3 为 *XY* 焦平面和包含光轴的 *XZ* 平面内聚焦光场强度的归一化分布以及三维光泡的光场强度归一化曲线实验结果。结果表明，三维光泡沿 *x* 方向边缘强度最大值与中心暗斑强度比值为 13.7:1，沿 *z* 方向的强度比值为 11.1:1，沿 *c* 方向的强度比值为 10.3:1，沿各方向的中心暗场半峰全宽分别为：$FWHM_x$=0.291 λ，$FWHM_z$=0.713 λ，$FWHM_c$=0.276 λ，光场强度均匀度 Φ= 87.3%。各实验结果与理论结果均较为吻合，实验误差主要来源于入射光场强度分布与理论预设间的差异，以及 RPC$_{detect}$ 对探测光的微量吸收与反射。与传统多光束合束方法相比，单光束矢量光场调控技术大大降低了实验系统搭建的复杂性，光学系统能量利用率约提升一倍。

4 总 结

针对目前采用多光束干涉叠加的方式来产生紧聚焦三维光泡所带来的光路复杂、不利于系统集成应用等问题，利用单光束矢量光场调控技术，在简易实验系统中产生了高强度均匀性的三维光泡，特别是针对脉冲光束，可以有效规避多光束合束所带来的光程补偿问题。此外，针对远场探测方式无法直接探测到聚焦光场的纵向偏振分量这一问题，利用探测光偏振转

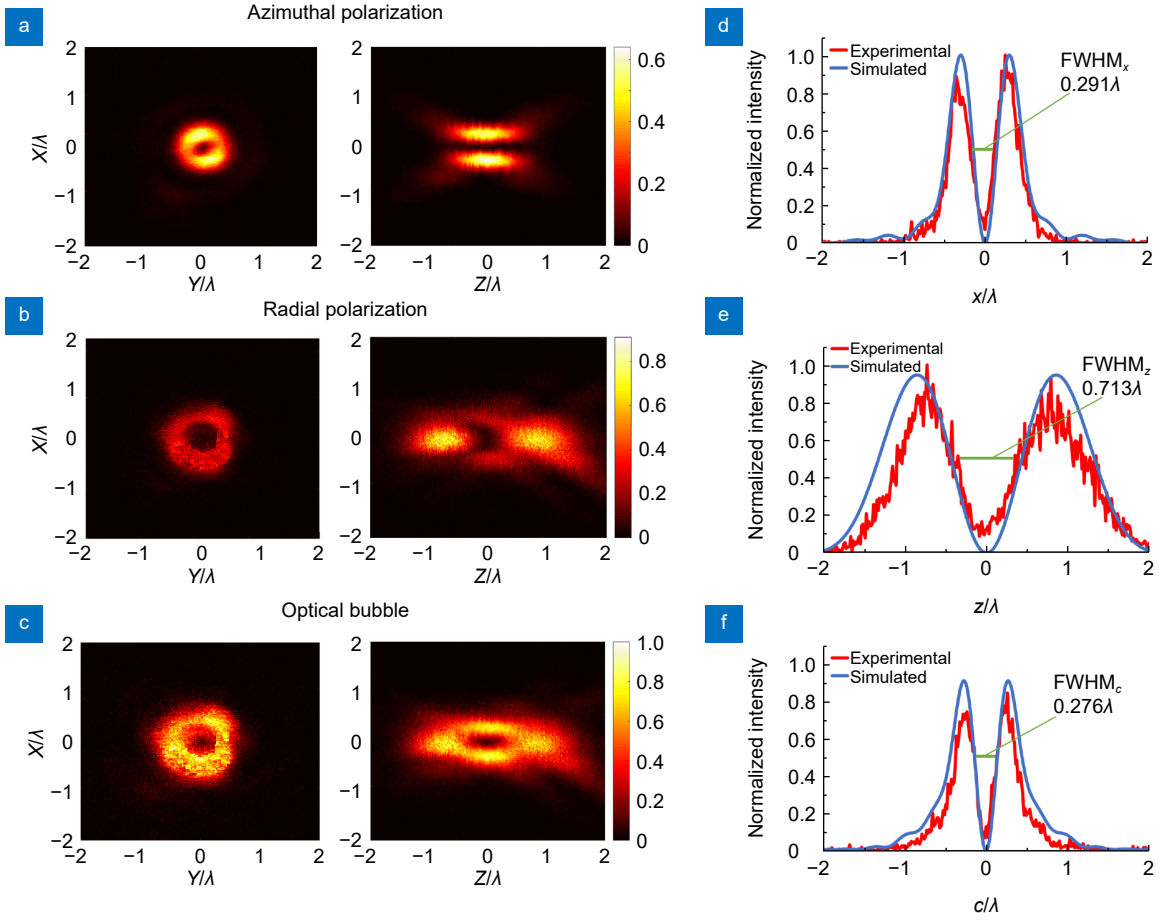

图 3 *XY* 焦平面和包含光轴的 *XZ* 平面内的光场强度归一化分布和三维光泡的光场强度归一化曲线实验结果。(a) 旋向偏振入射光紧聚焦生成中空管状光场; (b) 0/π 二元相位调制的径向偏振入射光紧聚焦光场; (c) 二者叠加生成的紧聚焦三维光泡; 三维光泡光场强度沿 (d) *x* 方向、(e) *z* 方向和 (f) *c* 方向的归一化曲线

Fig. 3 Experimental results of normalized intensity distributions of optical field in *XY* focal plane and *XZ* plane containing optical axis, as well as normalized intensity curves of three-dimensional optical bubble. (a) Tightly focused hollow tubular optical field generated by azimuthally polarized incident beam; (b) Tightly focused optical field generated by radially polarized incident beam with 0/π binary phase modulation; (c) Tightly focused optical bubble generated by the superposition of the two; Normalized intensity curves of three-dimensional optical bubble along (d) *x*-direction, (e) *z*-direction, and (f) *c*-direction

换技术，将径向偏振探测光转换成线偏振探测光，实现聚焦光场纵向偏振分量的间接测量，并合成产生三维光泡。通过调节旋向偏振入射光与 0/π 二元相位调制的径向偏振入射光的能量比，在实验上实现了边缘强度与中心暗斑强度比值大于 10:1、边缘强度均匀度接近 90% 的三维光泡，且与传统多光束合束方法相比，系统能量利用率约提升一倍，为双光束超分辨激光加工与光存储、粒子操控等领域提供了更为实用的技术途径。

利益冲突: 所有作者声明无利益冲突

参考文献

[1] Zhan Q W, Leger J R. Focus shaping using cylindrical vector beams[J]. *Opt Express*, 2002, **10**(7): 324−331.

[2] Moh K J, Yuan X C, Bu J, et al. Generating radial or azimuthal polarization by axial sampling of circularly polarized vortex beams[J]. *Appl Opt*, 2007, **46**(30): 7544−7551.

[3] Wang X L, Ding J P, Ni W J, et al. Generation of arbitrary vector beams with a spatial light modulator and a common path interferometric arrangement[J]. *Opt Lett*, 2007, **32**(24): 3549−3551.

[4] Ehmke T, Nitzsche T H, Knebl A, et al. Molecular orientation sensitive second harmonic microscopy by radially and azimuthally polarized light[J]. *Biomed Opt Express*, 2014, **5**(7): 2231−2246.

[5] Yu B Z, Wang J M, Wu T, et al. Optical rotation properties of TeO_2 crystal based on vector light field[J]. *J Appl Opt*, 2021, **42**(6): 963−968.
郁步昭, 王吉明, 吴彤, 等. 基于矢量光场的 TeO_2 晶体旋光特性研究[J]. 应用光学, 2021, **42**(6): 963−968.

[6] Biss D P, Youngworth K S, Brown T G. Dark-field imaging with cylindrical-vector beams[J]. *Appl Opt*, 2006, **45**(3): 470−479.

[7] Galiani S, Harke B, Vicidomini G, et al. Strategies to maximize

the performance of a STED microscope[J]. *Opt Express*, 2012, **20**(7): 7362−7374.

[8] Li C K, Li Y Z, Zhan Z Y, et al. Sub-diffraction dark spot localization microscopy[J]. *Photonics Res*, 2021, **9**(8): 1455−1461.

[9] Fischer J, Wegener M. Three - dimensional optical laser lithography beyond the diffraction limit[J]. *Laser Photonics Rev*, 2013, **7**(1): 22−44.

[10] Wollhofen R, Katzmann J, Hrelescu C, et al. 120 nm resolution and 55 nm structure size in STED-lithography[J]. *Opt Express*, 2013, **21**(9): 10831−10840.

[11] Wollhofen R, Buchegger B, Eder C, et al. Functional photoresists for sub-diffraction stimulated emission depletion lithography[J]. *Opt Mater Express*, 2017, **7**(7): 2538−2559.

[12] He X L, Li T L, Zhang J, et al. STED direct laser writing of 45 nm width nanowire[J]. *Micromachines*, 2019, **10**(11): 726.

[13] Qiu Y W, Ding C L, Zhan G Y, et al. Peripheral-photoinhibition-based direct laser writing with isotropic 30 nm feature size using a pseudo 3D hollow focus[J]. *Opt Laser Technol*, 2024, **170**: 110011.

[14] Liu X W, Xia X L, Yao Z F, et al. Theoretical and practical guide for an axial superresolved focus via Gouy phase steering[J]. *Photonics Res*, 2022, **10**(11): 2502−2512.

[15] Xie C, Liu T Y. Applications of vector vortex beams in laser micro-/nanomachining[J]. *Opto-Electron Eng*, 2024, **51**(8): 240089.
谢辰, 刘彤炎. 矢量涡旋光场在激光微纳加工中的应用[J]. 光电工程, 2024, **51**(8): 240089.

[16] Zijlstra P, Chon J W M, Gu M. Five-dimensional optical recording mediated by surface plasmons in gold nanorods[J]. *Nature*, 2009, **459**(7245): 410−413.

[17] Ouyang X, Xu Y, Xian M C, et al. Synthetic helical dichroism for six-dimensional optical orbital angular momentum multiplexing[J]. *Nat Photonics*, 2021, **15**(12): 901−907.

[18] Wang Z, Zhang B, Tan D Z, et al. Ostensibly perpetual optical data storage in glass with ultra-high stability and tailored photoluminescence[J]. *Opto-Electron. Adv.*, 2023, **6**(1): 220008.

[19] Ashkin A, Dziedzic J M, Bjorkholm J E, et al. Observation of a single-beam gradient force optical trap for dielectric particles[J]. *Opt lett*, 1986, **11**(5): 288−290.

[20] Ren Y T, Chen Q, He M J, et al. Plasmonic optical tweezers for particle manipulation: principles, methods, and applications[J]. *ACS Nano*, 2021, **15**(4): 6105−6128.

[21] Arlt J, Padgett M J. Generation of a beam with a dark focus surrounded by regions of higher intensity: the optical bottle beam[J]. *Opt Lett*, 2000, **25**(4): 191−193.

[22] Chen W B, Zhan Q W. Three-dimensional focus shaping with cylindrical vector beams[J]. *Opt Commun*, 2006, **265**(2): 411−417.

[23] Kozawa Y, Sato S. Focusing property of a double-ring-shaped radially polarized beam[J]. *Opt Lett*, 2006, **31**(6): 820−822.

[24] Bokor N, Davidson N. Generation of a hollow dark spherical spot by 4π focusing of a radially polarized Laguerre-Gaussian beam[J]. *Opt Lett*, 2006, **31**(2): 149−151.

[25] Bokor N, Davidson N. A three dimensional dark focal spot uniformly surrounded by light[J]. *Opt Commun*, 2007, **279**(2): 229−234.

[26] Xia X L, Zeng X Z, Song S C, et al. Longitudinal super-resolution spherical multi-focus array based on column vector light modulation[J]. *Opto-Electron Eng*, 2022, **49**(11): 220109.
夏小兰, 曾宪智, 宋世超, 等. 基于柱矢量光调控的纵向超分辨率准球形多焦点阵列[J]. 光电工程, 2022, **49**(11): 220109.

[27] Richards B, Wolf E. Electromagnetic diffraction in optical systems, II. Structure of the image field in an aplanatic system[J]. *Proc R Soc Lond A Math Phys Sci*, 1959, **253**(1274): 358−379.

[28] Youngworth K S, Brown T G. Focusing of high numerical aperture cylindrical-vector beams[J]. *Opt Express*, 2000, **7**(2): 77−87.

[29] Wang S C, Li X P. Wavefront manipulation of tightly focused cylindrical vector beams and its applications[J]. *Chin Opt*, 2016, **9**(2): 185−202.
王思聪, 李向平. 紧聚焦轴对称矢量光场波前调控及应用[J]. 中国光学, 2016, **9**(2): 185−202.

[30] Ouyang X, Xu Y, Xian M C, et al. Encoding disorder gold nanorods for multi-dimensional optical data storage[J]. *Opto-Electron Eng*, 2019, **46**(3): 180584.
欧阳旭, 徐毅, 冼铭聪, 等. 基于无序金纳米棒编码的多维光信息存储[J]. 光电工程, 2019, **46**(3): 180584.

[31] Li C H, Ouyang X, Sun J L, et al. Transverse scattering from nanodimers tunable with generalized cylindrical vector beams[J]. *Laser Photonics Rev*, 2023, **17**(6): 2200867.

[32] Ouyang X, Li C H, Cao Y Y, et al. Localized spontaneous chiroptical response in disordered plasmonic nanoaggregates[J]. *ACS Photonics*, 2023, **10**(7): 2407−2413.

[33] Xie X S, Chen Y Z, Yang K, et al. Harnessing the point-spread function for high-resolution far-field optical microscopy[J]. *Phys Rev Lett*, 2014, **113**(26): 263901.

作者简介

郑泽灿 (1999-)，男，硕士研究生，主要从事矢量光场调控领域的研究。

E-mail: authorzzc@stu2022.jnu.edn.cn

【通信作者】王思聪 (1987-)，男，博士，副研究员，博士生导师，主要从事矢量光场调控、光存储等领域的研究。

E-mail: wangsc@jnu.edn.cn

扫描二维码，获取PDF全文

Generation and detection of a tightly focused uniform optical bubble based on single-beam vector field modulation

Zheng Zecan, Wang Sicong*, Feng Jiahao, Zhou Zhikai, Chen Shukang, Song Shichao, Deng Zilan, Qin Fei, Cao Yaoyu, Li Xiangping

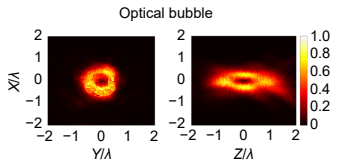

Experimental results of normalized intensity distributions of optical field in *XY* focal plane and *XZ* plane containing optical axis

Overview: Optical bubble, characterized by a tightly focused three-dimensional dark-field spot distribution, exhibits significant application values in fields such as optical manipulation and laser processing. Since 2000, research on the focused field distribution of optical bubbles has gradually gained attention. Arlt et al. generated an optical bubble in the focal region through the coherent superposition of two different Laguerre-Gaussian beam modes. Zhan et al. produced a tightly focused optical bubble using cylindrical vector beams combined with binary diffractive optical elements. Kozawa et al. achieved an optical bubble via coherent superposition of double annular radially polarized beams. However, the poor intensity uniformity at the edges of these generated bubbles limits their practical applicability. Bokor et al. utilized a Laguerre-Gaussian radially polarized beam for 4π focusing, generating an optical bubble with high intensity uniformity in the focal region. However, the counter-propagating focusing scheme in 4π focusing requires extremely high experimental alignment precision, making it challenging to implement in practice. Subsequently, this research group achieved the generation of an optical bubble with high intensity uniformity under conventional unidirectional focusing conditions by adjusting the energy ratio between an azimuthally polarized incident beam and a radially polarized incident beam modulated by a 0/π binary phase. Nevertheless, current experimental realizations of optical bubbles rely on multi-beam synthesis, which imposes stringent requirements on the experimental setup, particularly the multi-pulse beam synthesis system.

To address this issue, we utilize single-beam vector field modulation technology to generate an optical bubble with high intensity uniformity in a simplified experimental system. Furthermore, polarization conversion of the probe light enables the detection of individual polarization components within the focused field, facilitating the reconstruction of the three-dimensional morphology distribution of the optical bubble. By optimizing the energy ratio between the azimuthally polarized incident beam and the radially polarized incident beam modulated by a 0/π binary phase, we experimentally demonstrate an optical bubble with an edge-to-center dark spot intensity ratio exceeding 10:1 and edge intensity uniformity approaching 90%. Highly uniform optical bubble significantly enhances particle manipulation by enabling precise trapping of particles, thereby improving experimental controllability and repeatability. In terms of processing accuracy, it mitigates issues such as non-uniform machining depth and edge burrs, ultimately increasing production yield in material processing applications. Compared to traditional multi-beam synthesis methods, this technology markedly reduces system complexity while doubling optical energy utilization efficiency, providing a more practical technical approach for applications in dual-beam super-resolution laser processing, optical data storage, and particle manipulation.

Zheng Z C, Wang S C, Feng J H, et al. Generation and detection of a tightly focused uniform optical bubble based on single-beam vector field modulation[J]. *Opto-Electron Eng*, 2025, **52**(5): 250052; DOI: 10.12086/oee.2025.250052

Foundation item: National Key R&D Program of China (2023YFF0718101), National Natural Science Foundation of China (NSFC) (62375109, 62475102, 62275108)

Guangdong Provincial Key Laboratory of Optical Fiber Sensing and Communications, Institute of Photonics Technology, College of Physics & Optoelectronic Engineering, Jinan University, Guangzhou, Guangdong 510632, China

* E-mail: wangsc@jnu.edn.cn